Design and first results of the new divertor Thomson scattering diagnostic on ASDEX Upgrade

B. Kurzan, A. Lohs, G. Sellmair, M. Sochor, ASDEX Upgrade team

Max Planck Institute for Plasma Physics, Boltzmannstr. 2, 85748 Garching, Germany

Introduction

Divertor physics is a main field of interest at the ASDEX (Axial Symmetric Divertor Experiment) Upgrade tokamak. A new divertor Thomson scattering (DTS) system was installed with scattering volumes along a poloidal cord, which starts at the outer divertor plate, runs through the x-point and ends on the high field side.

Design of the DTS system

The regions of interest (ROIs), which are covered by the DTS system are the following (see fig. 1): (i) above the outer divertor leg (RL), (ii) the x-point (RX), and (iii) the high density front in the far scrape-off layer at the high field side (RH). Access to these regions defines the path of the laser beam, which is used as the light source for DTS. When the laser beam LB has entered the vacuum vessel it is deflected by mirror M3 to the plasma and ends at the beam dump BD. The Thomson scattered light is imaged by the collection lens CL to the fibers CF. A Nd-YAG laser with pulse energy 400 mJ and 20 Hz repetition rate is used. This small pulse energy is enough to obtain good scattering signals, but also reduces the risk to damage the beam optics inside the vacuum vessel, where access is difficult.

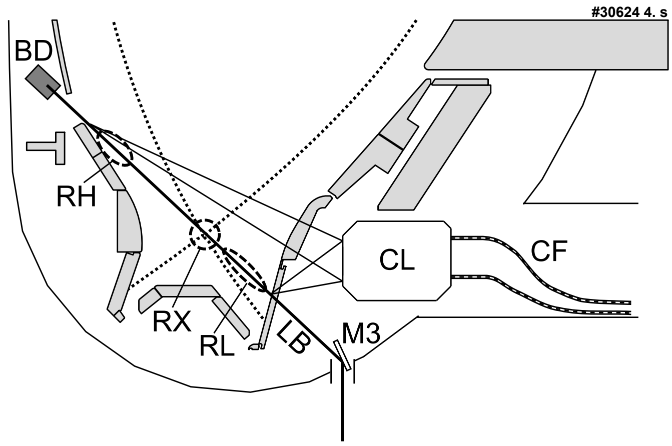

Figure 1: *Poloidal cross section of the scattering geometry. The laser beam LB runs over mirror M3 to the three ROIs (RL, RX, RH) and finally to the beam dump BD. The collection lens CL couples the scattered light to the fibers CF.*

Light collection path

The scattering volumes are seen by the collection lens within an angle of view of 45^o (see fig. 2). The Thomson scattered light is imaged onto fibers, which run parallel through the horizontal pump duct. To achieve this parallelisation of the optical path the collection lens has an image-side telecentric design.

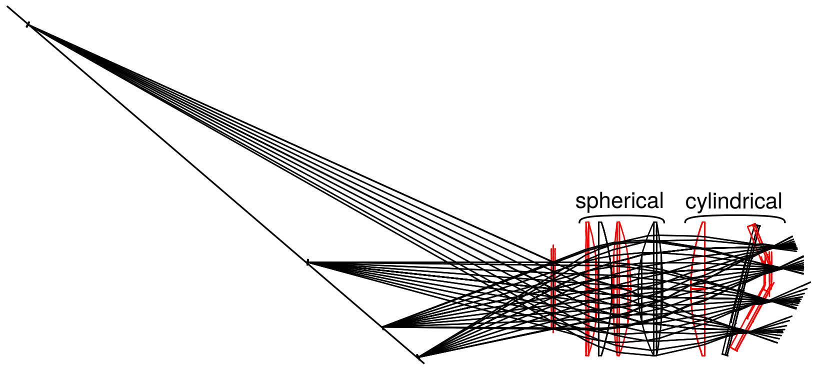

Figure 2: *Optical design of the collection lens.*

The collection lens is also anamorphic to image the ellipsoidal scattering volumes with length and width of around 1 cm, along the laser, onto circular fibers. So besides spherical, also cylindrical lenses are used. The convergence angle of the light path in front of the fibers can be up to 90^o. As an optically suitable fiber, which is radiation hard, and can be used in vacuum, a fiber with a silica core/ Teflon cladding and silicone buffer with 1000 μm diameter is used. After passing vacuum feedthroughs the fibers are fed to the polychromators. In total 24 working fibers and polychromators are available. For analysing the expected electron temperature range 1 - 100 eV, each polychromator has 4 spectral channels, covering the range 980 - 1062 nm (see fig. 3).

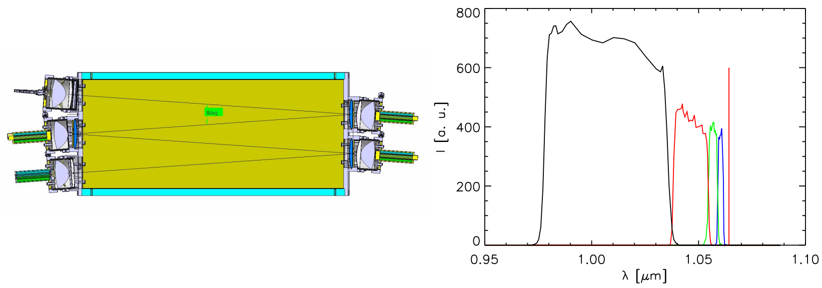

Figure 3: *Optical design of a polychromator and typical relative sensitivities of the spectral channels.*

Data acquisition

The signals of the detectors are recorded by newly developed data acquisition modules (1 GSamples/s, 14 bit resolution), which are tailored to fit the in-house data-link standard SIO2. With this high dynamic range both small and large signals can be recorded with the same amplifier sensitivity settings. This has advantages in (i) reducing systematic errors between Thomson scattering and calibration measurements, which have different signal amplitudes, and (ii) extending the range of temperature measurements beyond the design interval, for which large intensity ratio must be resolved.

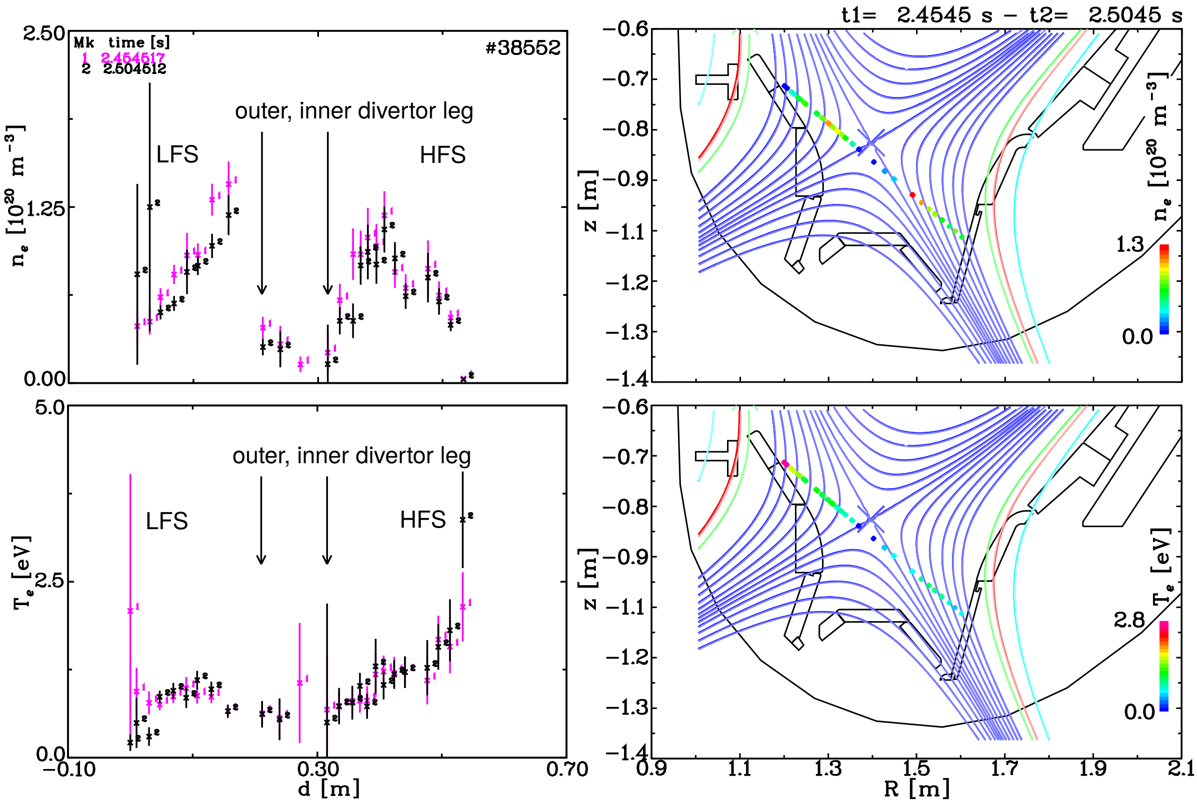

Figure 4: n_e *and* T_e *profiles versus laser coordinate d for a L mode plasma, and their mean values plotted at the positions of the scattering volumes in a poloidal cross section, where the magnetic flux surfaces are overlaid.*

Examples of measured profiles

The following two examples demonstrate the capabilities of the DTS system.

L mode

With the L mode discharge #38552 (line averaged density $\overline{n}_e$= 4.4 $\times$ 10^{19} m^{-3}, toroidal magnetic field B_t= -2.5 T, plasma current I_p= 600 kA, electron cyclotron resonance heating P_{ECRH}= 0.4 MW) the capability to measure small temperatures is shown. Profiles of electron density n_e and temperature T_e versus the coordinate d along the laser beam are shown in fig. 4. The laser beam enters the divertor on the low field side (LFS) at d$\approx$ 0.0 m. In fig. 4 also the profiles of electron density and temperature averaged over two time points are plotted in a poloidal plane at the positions of the scattering volumes together with the shape of the magnetic equilibrium. Towards the outer divertor leg the electron density is rising. In the private flux region between outer and inner divertor leg the electron density is low. On the high field side (HFS) high electron densities are measured. The electron temperatures are around 0.3 - 2 eV. This demonstrates that also electron temperatures below the specified range can be measured.

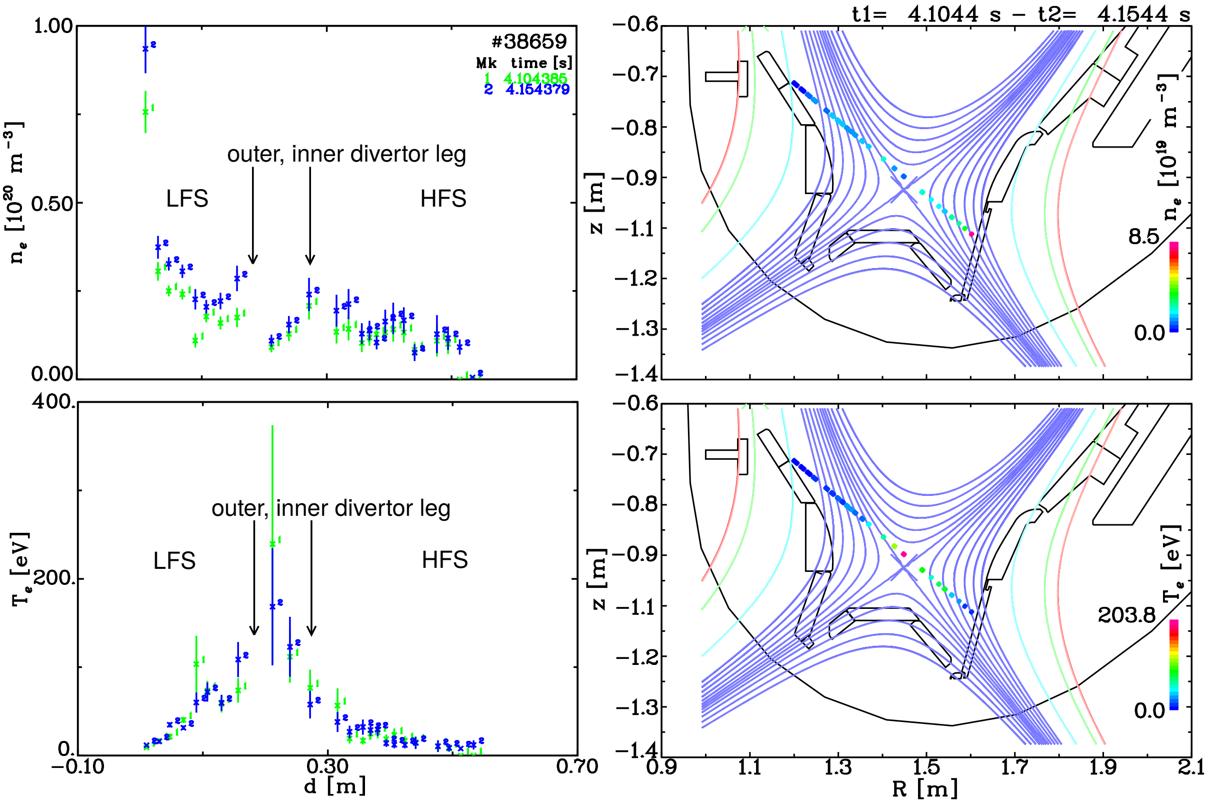

Figure 5: *n_e and T_e profiles versus laser coordinate d for a H mode plasma in reversed I_p, B_t, and their mean values plotted at the positions of the scattering volumes in a poloidal cross section, where the magnetic flux surfaces are overlaid.*

It was checked that the electron pressure along a flux surface measured with edge Thomson in the outer midplane, with divertor Thomson on the LFS and with Langmuir probes on the target is conserved.

H mode

The H mode discharge with shot number #38659 (line averaged density $\overline{n}_e$= 4.2 × 10^{19} m^{-3}, reversed toroidal magnetic field B_t= 2.4 T, and plasma current I_p= -810 kA, electron resonance heating P_{ECRH}= 1.5 MW, neutral beam injection heating P_{NBI}= 7.7 MW) is shown in fig. 5, because here electron temperatures up to 200 eV are measuered with DTS. This temperature is larger than the specified range. It is still possible to measure this, although with increased error bars.

Acknowledgement *This work has been carried out within the framework of the EUROfusion Consortium and has received funding from the Euratom research and training programme 2014-2018 and 2019-2020 under grant agreement No 633053. The views and opinions expressed herein do not necessarily reflect those of the European Commission.*